SUPPLEMENTAL MATERIAL

SUPPLEMENTAL METHODS

Patient eligibility

AMI was defined by chest pain lasting at least 20 minutes associated with electrocardiographic (ECG) changes (ST-segment elevation, new-onset left bundle branch block) and elevated cardiac enzyme levels. For inclusion, patients needed to be 18 years or older and able to give written informed consent. Eligibility for PET/MRI was defined as absence of pregnancy, hemodynamic stability, creatinine clearance >50ml/min, no allergy to gadolinium contrast agent, no claustrophobia, no pacemakers, ICDs or any other ferromagnetic material in the body.

SPECT imaging

After informed consent patients received 800 MBq of ^{99m}Tc-sestamibi intravenously. SPECT acquisition was performed 6 - 10 hours after PCI.

A dual head gamma camera (e.cam, Siemens Healthcare GmbH, Erlangen, Germany) with low-energy, high-resolution collimators was used for all ^{99m}Tc-sestamibi SPECT studies. Images were acquired in a 64-by-64 matrix; acquisition time per image was 40 seconds in 6° increments. Image data were subsequently reconstructed by use of a Butterworth filter with a cutoff frequency of 0.45, order 5. Central spatial resolution was 6.7 mm.[1]

PET/MR imaging

The performance of the Siemens Biograph mMR scanner has been previously evaluated in different studies.[2-4] Mean plasma glucose level was 97 ± 21 mg/dl. 145 ± 51 minutes after the intravenous injection of 317 ± 41 MBq of ^{18}F-FDG a list-mode PET scan in 3D mode was started. Correction of the emission data was performed for randoms, scatter, dead time and attenuation. The acquired images were reconstructed using a 3D attenuation-weighted ordered-subsets expectation maximization iterative reconstruction algorithm (AW-OSEM 3D) with three iterations and 21 subsets, Gaussian smoothing at 4 mm full-width at half-maximum, a matrix size of 344 x 344 and a zoom of 1.[3] Attenuation correction of the acquired PET data was accomplished using 2-point Dixon MR sequences as previously described.[5] Truncated parts of the body by the MR (due to the relatively small field of view) were recovered for the attenuation map from PET emission data using the so-called maximum likelihood reconstruction of attenuation and activity (MLAA) technique as previously described.[6] The spatial resolution of the PET component is according to prior studies about 5 mm.[2]

For assessment of late gadolinium enhancement (LGE) phase-sensitive inversion-recovery prepared T1-weighted gradient-echo pulse sequences (PSIR)[7] with an in plane resolution of 2 mm were acquired 10 min after the intravenous administration of 0.2 mmol Gadopentetat-Dimeglumin (Magnograf®; Marotrast GmbH, Jena, Germany) per kilogram body weight. Steady state free precession (SSFP) cine sequences were acquired to determine systolic function. ECG triggering was applied for image acquisition and all MRI images were obtained during breath hold. For the entire scan phased-array body surface coils were used.

Analysis of SPECT and PET images

Standardized uptake values (SUVs) normalized to the lean body mass were obtained as follows: First, in the area of myocardial infarction the maximum count rate was determined. Subsequently, a volume of interest (VOI) was automatically generated by region growing with a 50% threshold of the aforementioned maximum count rate. From this VOI mean SUVs (SUV_{mean}) and the volume of the VOI were automatically derived. The ^{18}F-FDG uptake extent was calculated by dividing the VOI volume by the volume of the left ventricle (derived from LGE MR images) and expressed as %LV. For the assessment of mean SUVs of remote myocardium fused images (summed ^{18}F-FDG PET + LGE MRI) were used. Mean SUVs were obtained by drawing manual regions into the myocardial wall opposing the infarct area on 3 consecutive slices. Analyses were performed using a dedicated commercial workstation and software (Syngo MMWP [workstation] and Syngo TrueD [software]; Siemens Medical Solutions).

In order to determine the spatial tracer distribution in the left ventricle, images of ^{99m}Tc-sestamibi and ^{18}F-FDG were first coregistered in this subset of patients. Then volumetric sampling of ^{18}F-FDG and ^{99m}Tc-sestamibi tracer distribution in the left ventricular myocardium was performed, and separate static polar maps of the coregistered ^{99m}Tc-sestamibi and ^{18}F-FDG images - each consisting of 460 segments - were created. In an automated process, the MunichHeart software then determined the maximal uptake of each tracer within the left ventricle and the polar maps were adjusted to this maximal value. Then, the size of the defect in the ^{99m}Tc-sestamibi polar map was automatically calculated (and expressed as %LV) by using a threshold of 50 percent (all segments <50%) – this threshold is derived from phantom studies as previously described.[8, 9] Accordingly, the ^{18}F-FDG uptake area was automatically derived by using a threshold of 50 percent (all segments >50%) and expressed as %LV.

For quantification of SUV_{mean} in the bone marrow, rectangular VOIs were drawn - guided by MR images - in the bone marrow of three consecutive vertebral bodies above the diaphragm. For quantification of SUV_{max} in the aorta, VOIs were placed on the ascending and descending aorta, guided by MRI. SUVs were normalized to the lean body mass. Analyses were performed using the Syngo MMWP workstation and Syngo TrueD software (Siemens).

LGE extent

First, the contours of the whole left ventricle were outlined on short-axis images using the MunichHeart (MR) software. Then, the extent of LGE in the whole LV myocardium was determined by manual delineation on short axis images and expressed as percentage of the left ventricle.[10]

Reagents for flow cytometry

EDTA anticoagulated whole blood was lysed in Versa Lyse (Beckman Coulter, CA, USA) for 10 minutes. Anti-human monoclonal fluorochrome-conjugated antibodies anti-CD45-ECD (clone J.33; Beckman Coulter, CA, USA), anti-CD14-PC5 (Clone RMO52; Beckman Coulter, CA, USA), anti-CD16-PC7 (Clone 3G8, Beckman Coulter, California, USA) and anti-CCR2-PE (Clone 48607, R&D Systems, Minnesota, USA) were used for staining of lysed whole blood. At least 50,000 Events were acquired for each patient sample on a Cytomics FC100 flow cytometer (Beckman Coulter, CA USA) and analyzed using Kaluza software (Beckman Coulter, CA, USA).

SUPPLEMENTAL FIGURE LEGENDS

Supplemental Figure 1. Segmental analysis of ^{18}F-FDG uptake in relation to LGE.

A: Mean and SD of SUV_{mean} in infarcted and remote myocardium, * $p<0.0001$ (left) and by-patient comparison of the ^{18}F-FDG uptake in the ischemically compromised coronary territory and the remote myocardium (right).

B: Segment based analysis of ^{18}F-FDG uptake and LGE transmurality. Results of visual scoring according to the AHA 17-segment model and intermethod comparison ($\kappa=0.63$) are shown. Segments were scored from 0-4 (LGE: 0 = no enhancement, 1 = ≤25% LGE extent, 2 = 25% to ≤50% LGE extent, 3 = 50% to ≤75% LGE extent, 4 = 75% to ≤100% LGE extent; ^{18}F-FDG: 0 = no uptake, 1 = mild ^{18}F-FDG uptake, 2 = moderate ^{18}F-FDG uptake, 3 = strong ^{18}F-FDG uptake or 4 = maximal ^{18}F-FDG uptake).

C: Correlation between the ^{18}F-FDG and LGE signal on a per patient basis (summed scores of ^{18}F-FDG and LGE).

D: Comparison of the frequency of ^{18}F-FDG uptake scores in LGE transmural and non-transmural segments.

Supplemental Figure 2. Post-ischemic ^{18}F-FDG uptake in the infarct area in relation to infarct size, peak leukocytes, CCR2+ monocytes and early monocyte subpopulations.

A: Sample dot plots from a representative patient demonstrating flow cytometric gating strategy. Monocytes were identified by typical forward (FSC)/side scatter (SSC) characteristics (left column, top). A gate was then set on the CD45+ population and monocytes were distinguished from granulocytes by CD14+ expression and SSC characteristics (center column, top and left column, bottom). CD16 expression was used to eliminate residual NK cells within the monocyte gate (center column bottom). Color back gating was used to ensure correct identification of monocytes in the CD45/SSC plot. Finally, monocyte subpopulations were defined by positive expression of CD16 (compared by isotype control) and high or low expression of CD14 within the predefined monocyte gate.

B: No correlation was found between post-ischemic ^{18}F-FDG uptake (SUV_{mean}) and LGE extent (top left), initial EF (top right), peak leukocytes (bottom left) and CCR2+ monocytes (bottom right).

C: Also, no correlation was found between post-ischemic ^{18}F-FDG uptake (SUV_{mean}) and $CD14^{high}CD16^{-}$ (inflammatory) (left), $CD14^{high}CD16^{+}$ (intermediate) (middle), and $CD14^{low}CD16^{+}$ (reparative) (right) monocyte subpopulations determined during the first 3 days after AMI. (G/L = 10^9 cells per liter)

Supplemental Figure 3. Change of LGE extent and global left ventricular function between initial and follow-up imaging.

A: The LGE extent decreased significantly between initial and follow-up imaging (*$p<0.0001$, left) in almost all patients (right).

B: There was no significant change in the EF between initial and follow-up imaging (left) due to diverse outcome in the different patients (right).

SUPPLEMENTAL FIGURES

Supplemental Figure 1

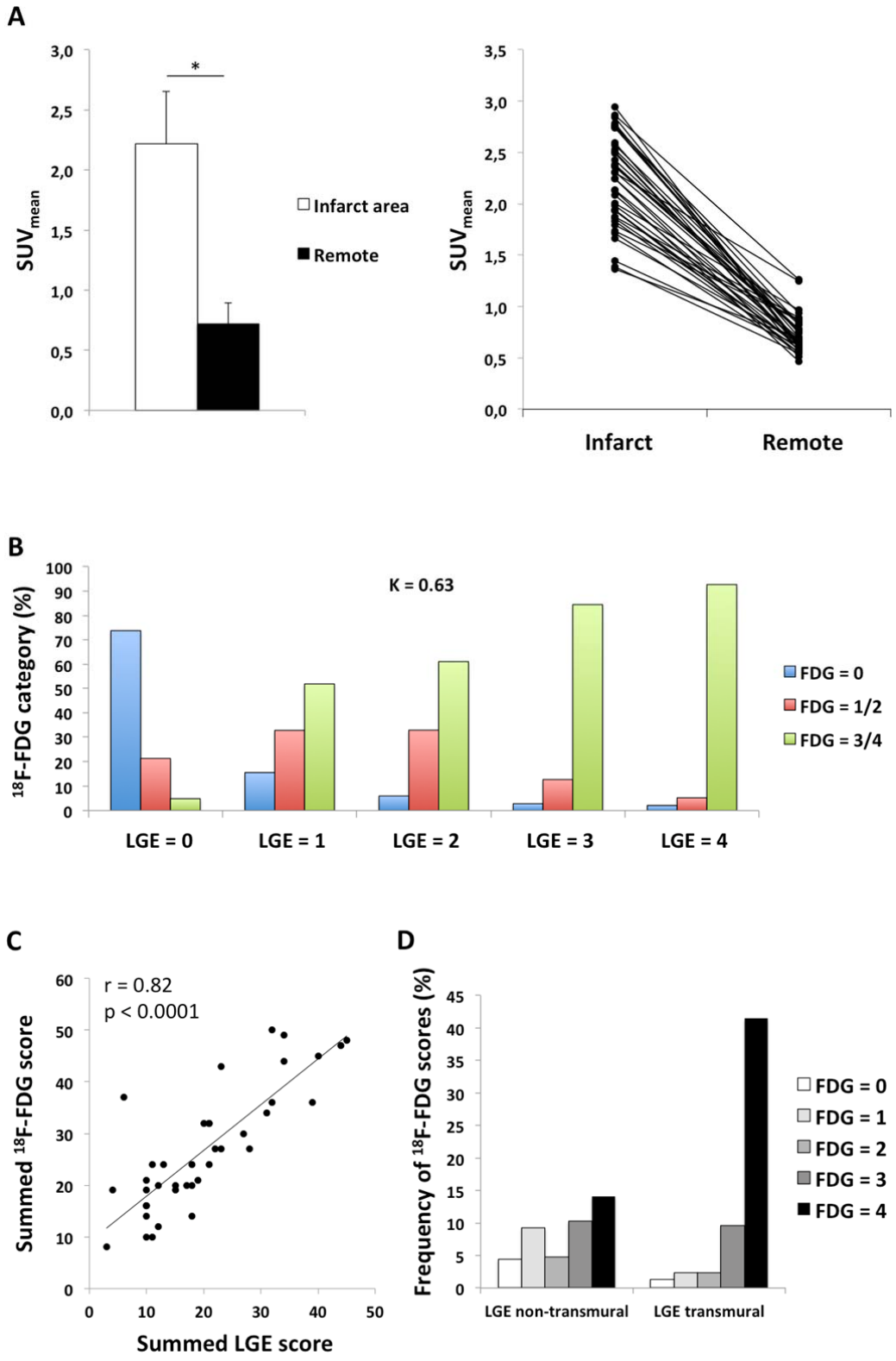

Supplemental Figure 2

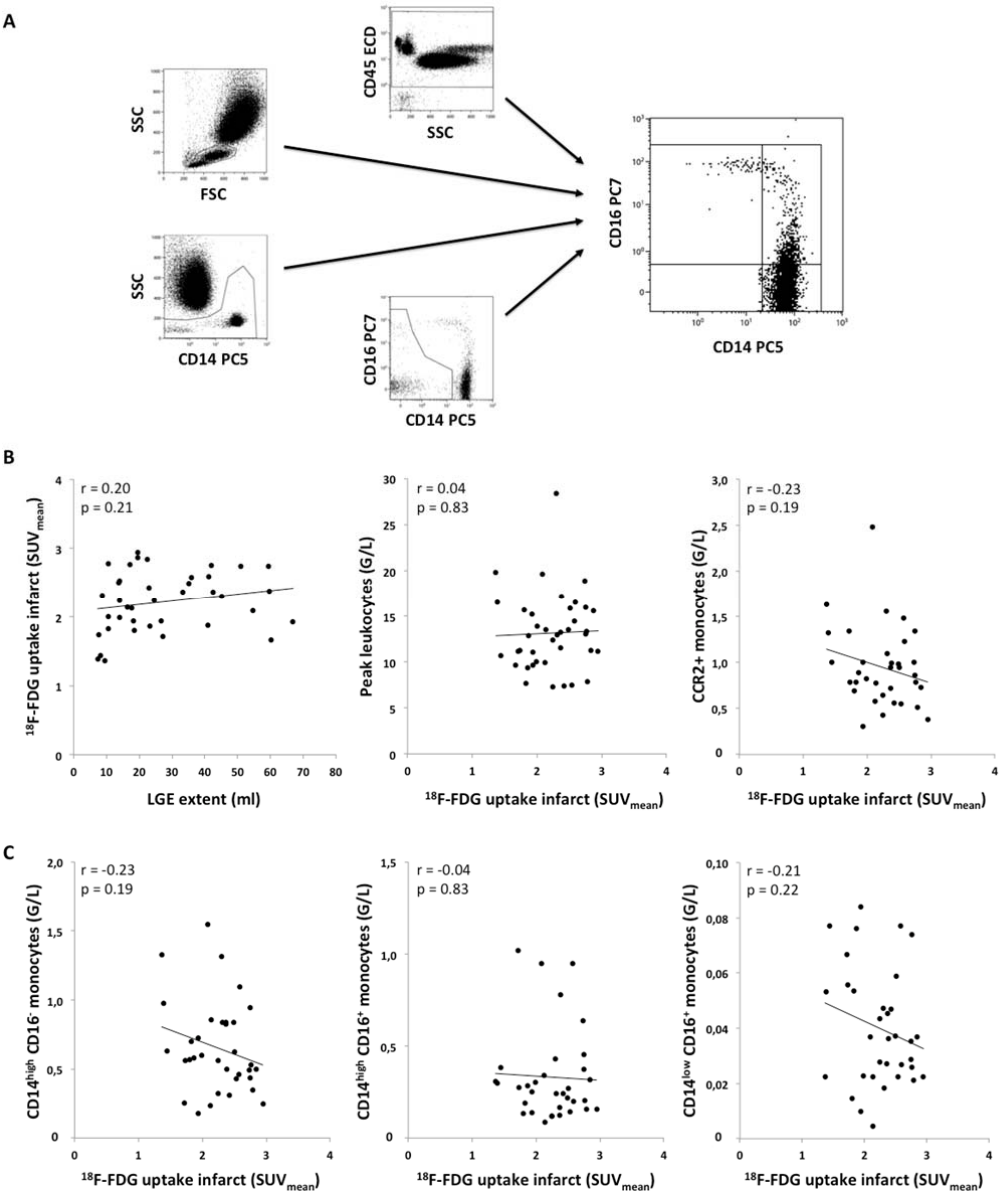

Supplemental Figure 3

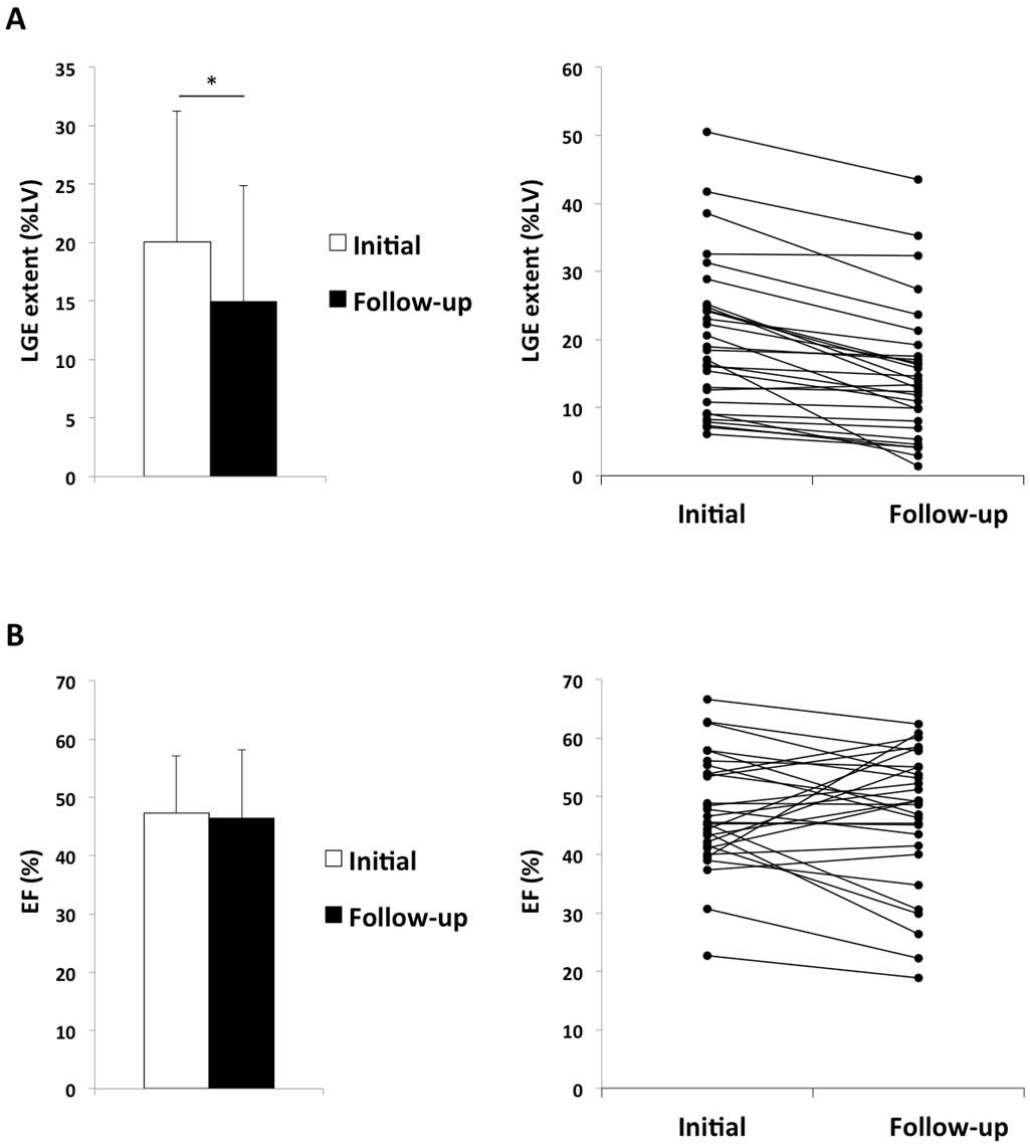

SUPPLEMENTAL REFERENCES

1. Imbert L, Poussier S, Franken PR, Songy B, Verger A, Morel O, Wolf D, Noel A, Karcher G and Marie PY. Compared performance of high-sensitivity cameras dedicated to myocardial perfusion SPECT: a comprehensive analysis of phantom and human images. *Journal of nuclear medicine : official publication, Society of Nuclear Medicine*. 2012;53:1897-903.
2. Delso G, Furst S, Jakoby B, Ladebeck R, Ganter C, Nekolla SG, Schwaiger M and Ziegler SI. Performance measurements of the Siemens mMR integrated whole-body PET/MR scanner. *Journal of nuclear medicine : official publication, Society of Nuclear Medicine*. 2011;52:1914-22.
3. Drzezga A, Souvatzoglou M, Eiber M, Beer AJ, Furst S, Martinez-Moller A, Nekolla SG, Ziegler S, Ganter C, Rummeny EJ and Schwaiger M. First clinical experience with integrated whole-body PET/MR: comparison to PET/CT in patients with oncologic diagnoses. *Journal of nuclear medicine : official publication, Society of Nuclear Medicine*. 2012;53:845-55.
4. Ibrahim T, Nekolla SG, Langwieser N, Rischpler C, Groha P, Laugwitz KL and Schwaiger M. Simultaneous positron emission tomography/magnetic resonance imaging identifies sustained regional abnormalities in cardiac metabolism and function in stress-induced transient midventricular ballooning syndrome: a variant of Takotsubo cardiomyopathy. *Circulation*. 2012;126:e324-6.
5. Martinez-Moller A, Souvatzoglou M, Delso G, Bundschuh RA, Chefd'hotel C, Ziegler SI, Navab N, Schwaiger M and Nekolla SG. Tissue classification as a potential approach for attenuation correction in whole-body PET/MRI: evaluation with PET/CT data. *Journal of nuclear medicine : official publication, Society of Nuclear Medicine*. 2009;50:520-6.
6. Nuyts J, Bal G, Kehren F, Fenchel M, Michel C and Watson C. Completion of a truncated attenuation image from the attenuated PET emission data. *IEEE transactions on medical imaging*. 2013;32:237-46.
7. Huber AM, Schoenberg SO, Hayes C, Spannagl B, Engelmann MG, Franz WM and Reiser MF. Phase-sensitive inversion-recovery MR imaging in the detection of myocardial infarction. *Radiology*. 2005;237:854-60.
8. Gibbons RJ, Verani MS, Behrenbeck T, Pellikka PA, O'Connor MK, Mahmarian JJ, Chesebro JH and Wackers FJ. Feasibility of tomographic 99mTc-hexakis-2-methoxy-2-methylpropyl-isonitrile imaging for the assessment of myocardial area at risk and the effect of treatment in acute myocardial infarction. *Circulation*. 1989;80:1277-86.
9. O'Connor MK, Gibbons RJ, Juni JE, O'Keefe J, Jr. and Ali A. Quantitative myocardial SPECT for infarct sizing: feasibility of a multicenter trial evaluated using a cardiac phantom. *Journal of nuclear medicine : official publication, Society of Nuclear Medicine*. 1995;36:1130-6.
10. Ibrahim T, Hackl T, Nekolla SG, Breuer M, Feldmair M, Schomig A and Schwaiger M. Acute myocardial infarction: serial cardiac MR imaging shows a decrease in delayed enhancement of the myocardium during the 1st week after reperfusion. *Radiology*. 2010;254:88-97.